

# Effect of Oxide Vacancies on Metal Island Nucleation

A. Bogicevic<sup>a</sup> and D. R. Jennison<sup>b</sup>

<sup>a</sup> *Ford Research Laboratory, MD 3083/SRL, Dearborn, MI 48124*

<sup>b</sup> *Surface and Interface Sciences Department, Sandia National Laboratories, Albuquerque, NM  
87185-1415, USA*

*(May 13, 2002)*

Point defects on oxide surfaces, presumably oxygen vacancies, are traditionally considered preferential nucleation centers for metal island formation. In a series of first-principles calculations for transition and noble metal nucleation on MgO(100), we show that the propensity for neutral anion vacancies to nucleate metal islands is strongly element dependent: To the right in a period, where *d*-shell filling is substantial, vacancies typically *inhibit* nucleation, whereas the opposite holds for far-left elements. This bears significant implications for the system-specific design of metal-oxide interface properties.

PACS number(s): 71.15.Mb, 68.35.-a

*Keywords: Metal island nucleation; Surface defects; oxygen vacancies; density-functional theory*

Corresponding author: Alexander Bogicevic

Scientific Research Laboratories, Ford Motor Company

Dearborn, MI 48124, USA

Phone: +1 313 845-8625, FAX: +1 313 322-7044, E-mail: abogicev@ford.com

The tremendous growth of practical applications based on oxide-supported metal aggregates is rapidly coming to a point where further advances rest on precise atomic-level control of the metal-oxide interface. This is particularly appreciable in the ever-shrinking world of microelectronics components, where device performance depends on metal-oxide junctions often only a few atomic layers thick. At this nano-scale, new physical phenomena have also been reported, including the sudden onset of catalytic activity of normally inert metals [1]. By controlling the nature and density of point defects on oxide surfaces, one envisions a novel means of tailoring wetting, adhesion, and dispersion of metal particles and films for specific applications [2,3]. Such an advantage in technological processing requires that we understand how defects affect the nucleation and growth of elementally differing metal overlayers. Despite significant experimental and theoretical efforts, there is still no consensus as to the nature of the point defects in nominally “clean” systems, nor is there any clear understanding of observed metal species variations. A number of studies have shown that single surface vacancies often strongly trap metal adatoms (and many other non-metals), but the understanding of metal island nucleation requires knowledge of how these trapped adatoms in turn react to subsequent metal adatoms. Very little is known about this subject.

In this Letter, we show that the propensity of oxygen vacancies ( $F_s$  centers) to nucleate metal islands is decided primarily by the degree of  $d$ -shell filling: the charge transfer from the defect to the metal weakens the adsorbate-adsorbate bond for metals with greater than half filled shells, reducing the stability of the metal dimer. To the left in the periodic table, the opposite effect is observed as the  $d$ -shell filling is decreased. The tendency for anion vacancies to promote or inhibit nucleation is thus strongly system dependent, and cannot be explained just by studying how single adatoms interact with the defect contra the clean terrace. This provides significant insight for understanding and ultimately manipulating metal-oxide interface properties via selective control of defect density using, e.g., common electron and photon techniques to make vacancies. We also compare our calculations with kinetic models of experimental studies on cluster nucleation.

## I. THEORETICAL APPROACH

Our calculations are based on density-functional theory (DFT) [4,5], with core-electron interactions mediated by pseudopotentials, as implemented in the VASP code [6]. The generalized gradient approximation (GGA) [7] is chosen for the exchange-correlation functional in order to treat most accurately the relatively weak dimer covalent bonds. The one-electron wave functions are expanded in a plane-wave basis with an energy cutoff of 20 Ry, using ultra-soft Vanderbilt pseudopotentials [8]. The Kohn-Sham equations are solved iteratively, and the atomic structure is optimized until the forces on all unconstrained atoms are less than 0.03 eV/Å. The super-cell is constructed of five MgO(100) layers containing 36 atoms each (Fig. 1). The bottom two layers are fixed at bulk positions, while all other atoms are allowed to fully relax. Adsorbates and defects are situated on the top side of the slab with at least 15 Å of vacuum separation to the nearest periodic image cell. The Brillouin zone is sampled using a  $(2 \times 2 \times 1)$  **k**-point mesh.

The electronic structure and atomic relaxations of isolated oxygen and magnesium vacancies have been described in a previous study by us [9], and by others [10,11]. The removal of a neutral oxygen produces an  $F_s$  center, where two electrons are weakly trapped by the electrostatic Madelung potential. In the case of cation removal, the two electron holes of the  $V_s$  center are distributed mainly over the four nearest neighbor in-plane anions. The interaction between two neighboring oxygen vacancies is negligible (10 meV attraction) [9], whereas the binding of  $F_s$  and  $V_s$  vacancies is found to be very strong (5.49 eV; experimentally 5.2 eV [9]). Although other types of surface defects exist, e.g. charged paramagnetic anion vacancies, our calculations and conclusions are limited to charge-neutral  $F_s$  oxygen vacancies.

## II. NUCLEATION ON THE TERRACE AND AT DEFECTS

Under typical growth conditions, pairs of atoms, or dimers, constitute the first step in island nucleation [12], and are therefore central to the growth of metal clusters and films on oxides (larger clusters are discussed below). It has repeatedly been observed for different metal-oxide systems that nucleation of metal islands at moderate temperatures is governed by point defects [13]. A plausible reason for this is that the adatom-adatom binding on defect-free terraces is too weak to prevent rapid dimer dissociation, and that the role of surface defects is to stabilize island formation by enhancing the addimer binding energy  $E_b$ . Recently, we showed that the Pt dimer bond is considerably weakened at both  $F_s$  and  $V_s$  centers on MgO(100), but strongly strengthened at ad-OH impurities [9], which would serve as nucleation centers, as observed experimentally for other systems [14]. This result poses two important questions: (i) what is the mechanism behind this bond weakening at the common  $F_s$  centers, and (ii) how general is this result?

In this study, we examine the binding of isolated adatoms and metal dimers on the clean terrace and at oxygen vacancies for Nb, Ru, Rh, Pd, Ag, Ir, Pt, and Au on MgO(100). All calculations are performed spin-unpolarized, so that spin effects, i.e. mainly the effects of the specific states of isolated atoms and molecules, are removed. As a test, fully spin-polarized calculations were performed for the Rh/MgO system. Although net spin moments persist upon adsorption, the total energies are only weakly affected, by a few tens of meV's typically, and at most 0.30 eV. Spin polarization effects are thus relatively weak when compared to the energetics of charge transfer into bonding/non-bonding  $d$ -orbitals, as shown below. In the single atom adsorption calculations, the actual coverage due to periodic boundary conditions is 1/36 ML (at low coverages, atoms occupy both anion and cation sites). For all practical purposes, the adatoms can therefore be considered isolated.

### A. Trapping of single adatoms

The atomic adsorption energies on the terrace and at  $F_s$  centers are summarized in Table I. Examining this compilation of data, we first note that the trends for atomic binding across the second and third transition metal series agree well with previous studies by us on model ultrathin alumina films [15], and by Yudanov *et al.* on MgO(100) [16]. In both systems, beginning with the noble metals, the atomic adsorption increases monotonically to the left in the periodic table, at least until it reaches Group V.

The atomic binding at oxygen vacancies is significantly stronger than on terraces, by about 1-4 eV, mainly due to electron transfer from the  $F_s$  color center to the adatom and the attendant electrostatic interactions with the oxide. The stronger binding at these defects shortens the adatom-surface bond, so that adatoms sit on average about half an Å closer to the surface (Table II). We note that the binding trend is not nearly so pronounced at the vacancy, where atomic adsorption energies for the second and third Group VIII columns are quite similar.

### B. Metal dimerization

In the dimer calculations, care must be taken to ensure that the minimum-energy configuration is reached. Besides optimizing the atomic positions of the two atoms, the two space angles  $\theta$  and  $\phi$  also need to be determined. Because of relatively soft bending and twisting modes, the extraction of the latter two parameters is by far the most computer intensive. In the dimer calculations, we start out with three different configurations: an (almost) upright dimer ( $\theta \simeq 0^\circ$ ,  $\phi \simeq 0^\circ$ ), a dimer tilted towards a neighboring cation ( $\theta > 0^\circ$ ,  $\phi \simeq 0^\circ$ ), and a horizontal dimer ( $\theta \simeq 90^\circ$ ,  $\phi \simeq 0^\circ$ ). A slight off-symmetry in the starting configurations is imposed to force a break of symmetry. The calculations show that dimers at the vacancies prefer to tilt towards surface cations rather than anions, suggesting transferred charge from the vacancy is sufficient to cause both dimer atoms to be negatively charged. Thus, we

limit ourselves to the case of  $\phi \simeq 0$ . The dimer atoms (and the topmost three slab layers) are then allowed to fully relax as described above. The dimer binding energy on the clean terrace is defined as  $E_b = E_2 + E_0 - 2E_1$ , where  $E_2$  is the total energy for the adsorbed dimer,  $E_0$  is the energy of the clean slab, and  $E_1$  is the energy for the isolated adatom, and thus measures the tendency for dimer dissociation on the surface. The dimer binding energy at the  $F_s$  defect is similarly defined as  $E_b^v = E_2^v + E_0 - E_1 - E_1^v$ , where the superscript  $v$  indicates adsorption energies at the defect.

Returning to Table I, we note that the dimer (adatom-adatom) binding on the terrace increases to the left in the periodic table, and that there is a general weakening of the dimer bond upon adsorption at oxygen vacancies except for noble metals. With respect to dimer binding trends at the vacancies, we note differences in the second and third row transition metal elements, while the noble metals in contrast behave similarly. From this data, it should be absolutely clear that although adatom and dimer binding is intercoupled, adatom bonding alone cannot explain dimer energetics. Obviously, the influence of  $F_s$  centers on dimer binding is complex, much more so than previously anticipated, which emphasizes the need for accurate (quantum-mechanical) theoretical studies.

We believe an understanding of these complex trends can be had from simple shell filling arguments. At the vacancy, electron density is accepted by the metal. This is evident from a lengthening of the adatom-adatom bond (see below), by the dimer tilt angles being towards neighboring cations, and from a direct charge density analysis (not shown). In Group VIII elements, this adds to antibonding levels because the  $d$ -shells are overfull, weakening the adatom-adatom bonds. In contrast, the opposite happens to the far left in the periodic table (Nb) where added electron density to the underfilled  $d$ -shell strengthens the dimer bond. Due to severe converge problems caused by molecular levels being close to the conduction band, the Nb results are only approximate in energy and not listed in geometry. The noble metals bind only weakly to the oxide, and their dimers are less prone to interact with the  $F_s$  defects. This results in a weak perturbation of the dimer bond due to lesser charge exchange, as attested by the dimer bond strengths being quite near gas phase values (e.g. 1.7 eV for

Ag [17]).

As the second adatom attaches to the first one, the atoms rise out of the surface by a few tenths Å (Table II) both on the clean terrace and at the oxygen vacancy. An exception is the Nb adatom. The reason for the general trend is that the metal-metal bond normally is formed at the expense of the metal-oxide bond. Comparing dimer geometries on the terrace and at the  $F_s$  center, we note that the dimer sits notably lower at the defect, and that its metal-metal bond in most cases is lengthened. This effect arises as charge is donated to the adsorbate, resulting in a weaker and longer adatom-adatom bond.

Before turning to the island nucleation aspects of our results, we note that our results for the Ag dimer binding energy is in numerical disagreement with the result of Ferrari *et al.* [17]. In this DFT study, the authors reported a pronounced decrease in surface dimer binding compared with the gas phase. One possible explanation is that the symmetry impositions and geometry in this work were restricted, with the axis of the Ag dimer perpendicular to the surface above an anion site. In contrast, we find an appreciable tilt of  $16^\circ$  upon relaxation and a subsequent strengthening of the dimer bond compared with upright adsorption. Thus, the earlier study may have missed the ground state.

### III. DISCUSSION

Whether or not the calculated changes in dimer binding are important in a growth experiment depends on the growth conditions. For example, a change in  $E_b$  of, say, 1 eV on top of an already strong dimer bond will not affect the nucleation process and surface morphology at low temperatures and moderate fluxes; once two atoms meet, they will stick together for a sufficiently long time to nucleate an island, irrespective of the actual dimer binding energy. Conversely, it is easy to see that the same change in a relatively weak dimer bond should have a much greater effect. At high enough temperatures, all changes in dimer binding will be important.

Focusing on the specific results of this study, we conclude that at low to moderate

temperatures, the defect density should play an important role for mainly Pd, Rh, Ir, and Pt, simply because the relative change  $\Delta E_b/E_b$  is the greatest for these systems. In the case of Pd, the  $F_s$  center actually stabilizes a (weak) repulsive interaction of two adatoms, whereas in the case of Pt, the same defect strongly destabilizes the nominally attractive interactions between two adatoms.

Although the dimer binding energy is arguably one of the most important quantities that govern the nucleation of metal islands, the subsequent growth into larger aggregates and films also depends on the formation energies of trimers, tetramers, etc. Once again, the main question here is how oxygen vacancies affect cluster formation. As an initial study into this question, we have taken a closer look at the trimer formation of Pd atoms on MgO(100). Interestingly enough, although  $\text{Pd}_3$  is basically unstable on the clean terrace ( $E_b = 0.05$  eV with respect to a dimer and a monomer), it is strongly stabilized by the oxygen vacancy, where  $E_b = 0.66$  eV. This stabilization of trimers at oxygen vacancies should be important at lower temperatures, simply because the dimer itself is quite unstable (with or without defects near). We also make a note of our observation that at low coverages, below about half a ML, metal adatoms occupy both anion and cation sites, whereas at higher coverages a transition is observed to encompass anion-only adsorption.

At this point, we turn our focus to comparisons with experimental studies. Recent atomic-force microscopy measurements for growth of Pd clusters on MgO(100) at a temperature of 200-800 K were performed and interpreted using mean-field nucleation theory by Haas and coworkers [18]. The fact that the island density stays constant over a wide span of deposition temperatures is characteristic of defect controlled nucleation (steps were eliminated as primary nucleation centers using the micrographs). The mean-field model parameters that best reproduced the experimental data encompassed an atomic adsorption energy on the clean terrace (our computed values in parentheses)  $E_a \simeq 1.2$  eV ( $E_a = 1.37$  eV), a trapping energy at the defect, presumably oxygen vacancies,  $\Delta E_a > 1.2$  eV ( $\Delta E_a = 2.72$  eV), atomic diffusion barrier on the clean terrace  $E_d < 0.3$  eV ( $E_d = 0.86$  eV), and a dimer binding energy  $E_b \simeq 1.2$  eV ( $E_b = -0.03$  eV;  $E_b^v = 0.09$  eV). Clearly, there is a large dis-



agreement between our results and the mean-field model regarding the diffusivity of isolated adatom and the dimer binding energy. Given the incorporation of gradient corrections and the use of accurate nudged-elastic-band methods for the transition-state search, it is hard to write off such large discrepancies to numerical errors.

Our results indicate that the reason such a small diffusion barrier is needed in the mean-field model to reproduce the experimental data is to account for the fact that no nucleation was noted between defects [18]. Our calculations suggest that this observation should instead be attributed to the fact that the critical nucleus size for this system is in fact  $i = 2$ , and that the reason no nucleation is seen between defects is that dimers are unstable at the experimental temperatures and will not nucleate new islands on the clean surface or at the defects.

In conclusion, we present a detailed systematic study of metal adatom and dimer binding on clean MgO(100) terraces and at oxygen vacancy defects using highly accurate first-principles calculations. These results demonstrate complex variations in adatom and ad-dimer binding across the periodic table. Using these data, we develop a conceptually simple  $d$ -shell filling model to explain these variations, and in particular the propensity for  $F_s$  vacancies to nucleate or inhibit metal island formation. This information provides a useful basis for devising element-specific defect density control strategies to tailor metal-oxide interfaces.

The authors wish to thank Prof. Gianfranco Pacchioni for discussions and for providing unpublished information. Sandia is a multiprogram laboratory operated by Sandia Corporation, a Lockheed Martin Company, for the United States Department of Energy under contract DE-AC04-94-AL85000.

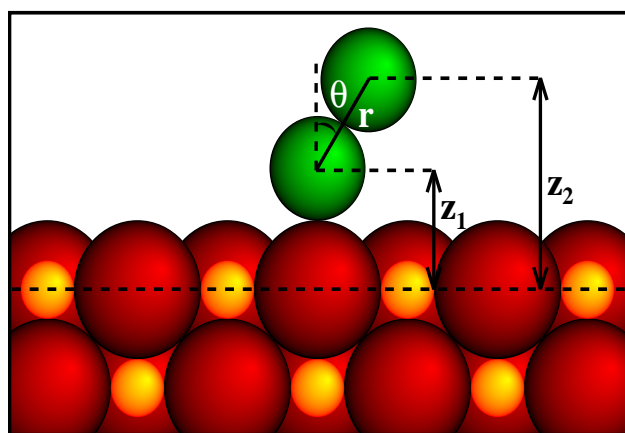
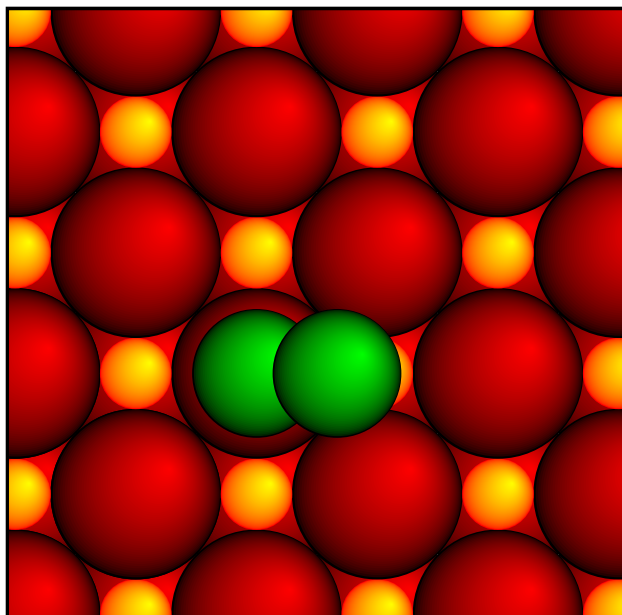
## REFERENCES

- [1] M. Valden, X. Lai, and D. W. Goodman, *Science* **281**, 5383 (1998).
- [2] C. Niu, K. Shepard, D. Martini, J. A. Kelber, D. R. Jennison, and A. Bogicevic, *Surf. Sci.* **465**, 163 (2000).
- [3] Y. F. Zhukovskii, E. A. Kotomin, P. W. M. Jacobs, and A. M. Stoneham, *Phys. Rev. Lett.* **84**, 1256 (2000).
- [4] P. Hohenberg and W. Kohn, *Phys. Rev.* **136**, B864 (1964).
- [5] W. Kohn and L. J. Sham, *Phys. Rev.* **140**, A1133 (1965).
- [6] G. Kresse and J. Hafner, *Phys. Rev. B* **47**, 558 (1993); **49**, 14251 (1994); **54**, 11169 (1996).
- [7] J. P. Perdew *et al.*, *Phys. Rev. B*, **46**, 6671 (1992).
- [8] D. Vanderbilt, *Phys. Rev. B* **32**, 8412 (1985); **41**, 7892 (1990).
- [9] A. Bogicevic and D. R. Jennison, *Surf. Sci. Lett.* **437**, L741 (1999).
- [10] A. M. Ferrari and G. Pacchioni, *J. Phys. Chem.* **100**, 9032 (1996).
- [11] P. V. Sushko *et al.*, *Surf. Sci.* **450**, 153 (2000) and references therein.
- [12] H. Brune, *Surf. Sci. Rep.* **31**, 121 (1998).
- [13] Recent examples include M. Bäumer *et al.*, *Surf. Sci.* **454-456**, 957 (2000); M. Frank *et al.*, *ibid.* **454-456**, 968 (2000).
- [14] G. Ertl and H.-J. Freund, *Phys. Today* **52**, 32 (1999).
- [15] A. Bogicevic and D. R. Jennison, *Phys. Rev. Lett.* **82**, 4050 (1999).
- [16] I. Yudanov, G. Pacchioni, K. Neyman, and N. Rösch, *J. Phys. Chem B* **101**, 2786 (1997).

- [17] A. M. Ferrari, C. Y. Xiao, K. M. Neyman, G. Pacchioni, and N. Rösch, Phys. Chem. Chem. Phys. **1**, 4655 (1999).
- [18] G. Haas, A. Menck, H. Brune, J. V. Barth, J. A. Venable, and K. Kern, Phys. Rev. B **61**, 11105 (2000).

## FIGURES

FIG. 1. Top and side views of the MgO(100) surface. The adsorption heights  $z_1$  and  $z_2$  are defined with respect to the average positions of the topmost surface layer atoms. The dimer tilt  $\theta$  is defined with respect to the surface normal, and  $r$  is the length of the addimer. (Small spheres represent Mg.)



# TABLES

TABLE I. Calculated GGA energies in eV for selected noble and transition metals: adsorption energy on the clean terrace ( $E_a$ ), adsorption energy at the oxygen vacancy ( $E_a^v$ ), and increase in adsorption energy  $\Delta E_a = E_a^v - E_a$ . The next three lines concern the dimer binding energy on the clean terrace ( $E_b$ ), same with one of the dimer atoms in the  $F_s$  center, and the difference in dimer binding  $\Delta E_b = E_b^v - E_b$ .

	$E_a$	$E_a^v$	$\Delta E_a$	$E_b$	$E_b^v$	$\Delta E_b$
Nb	3.22	3.00	-0.22	5.4	6.4	+ 1.0
Ru	2.40	4.33	+1.93	4.50	3.31	-1.19
Rh	1.93	4.32	+2.39	1.47	1.09	-0.37
Pd	1.34	4.06	+2.72	-0.03	0.09	+0.13
Ag	0.53	1.80	+1.27	1.81	1.86	+0.05
Ir	3.19	6.26	+3.08	2.79	1.38	-1.42
Pt	2.67	6.49	+3.83	0.72	-0.14	-0.86
Au	0.90	3.12	+2.22	2.15	2.21	+0.06

TABLE II. Compilation of fully relaxed adsorption heights of single metal atoms and dimers on the clean terrace and at the  $F_s$  center (superscript  $v$ ) in Å. The dimer tilt  $\theta$  is given with respect to the normal, and the unit is degrees.

	Atom		Dimer							
	$z_1$	$z_1^v$	$z_1$	$z_2$	$r$	$\theta$	$z_1^v$	$z_2^v$	$r^v$	$\theta^v$
Nb	2.04	2.05	—	—	—	-	—	—	—	-
Ru	1.98	1.62	2.17	4.13	1.96	0.1	1.96	2.85	2.01	63.8
Rh	2.01	1.51	2.37	4.55	2.18	0.2	1.65	2.78	2.34	61.1
Pd	2.06	1.42	2.10	2.65	2.63	77.9	1.50	2.84	2.57	58.5
Ag	2.43	1.91	2.37	4.85	2.58	16.2	1.74	3.25	2.71	56.2
Ir	1.95	1.44	2.06	4.26	2.20	0.2	1.67	2.84	2.28	59.2
Pt	1.99	1.62	2.06	4.42	2.36	0.0	1.52	2.83	2.50	58.3
Au	2.34	1.65	2.18	4.71	2.53	0.2	1.53	3.04	2.72	56.3